Journal of
Synchrotron
Radiation
ISSN 1600-5775

Profile etching for prefiguring X-ray mirrors

Chian Liu,* Jun Qian and Lahsen Assoufid

X-ray Science Division, Argonne National Laboratory, 9700 South Cass Avenue, Argonne, IL 60439, USA.
*E-mail: cliu@aps.anl.gov

Received 20 October 2014
Accepted 12 January 2015

A method to pre-shape mirror substrates through etching with a broad-beam ion source and a contoured mask is presented. A 100 mm-long elliptical cylinder substrate was obtained from a super-polished flat Si substrate with a 48 nm root-mean-square (r.m.s.) figure error and a 1.5 Å r.m.s. roughness after one profile-etching process at a beam voltage of 600 V without iteration. A follow-up profile coating can be used to achieve a final mirror. Profile etching and profile coating combined provide an economic way to make X-ray optics, such as nested Kirkpatrick–Baez mirrors.

© 2015 International Union of Crystallography

Keywords: broad-beam ion figuring; ion etching; profile coating; nested KB mirrors.

1. Introduction

For the past 15 years, profile coating has been an essential technique in our laboratory for making laterally graded multilayers, monolithic and nested Kirkpatrick–Baez (KB) mirrors, multilayer Laue lenses, and X-ray gratings using multilayers grown on staircase substrates (Liu *et al.*, 2001, 2003, 2012*a*; Kang *et al.*, 2006; Wen *et al.*, 2013). KB mirrors with sub-nanometre figure errors are routinely produced using flat Si substrates with only two profile-coating iterations (Kewish *et al.*, 2010). When a flat substrate is converted into an elliptical mirror by coating alone, the substantial film thickness and gradient can produce non-uniform film stress and may fail under extreme X-ray irradiations, owing to possible film stress relaxation (Liu *et al.*, 2012*b*). If a spherical substrate is used, the cross-section profiles will be different. A precise elliptical cylinder profile is important in the fabrication of nested KB mirrors, where the side edge of one mirror is polished and aligned on another identical mirror (Liu *et al.*, 2012*a*). It is critical to have the same elliptical profile at whatever polishing depth.

Ion beam figuring (IBF) has been developed rapidly in the past 40 years to meet the increasing demands on high-quality optical components. Sophisticated IBF machines with multi-axis computer-controlled systems are available, but costly. Application of IBF to X-ray mirrors was introduced to the synchrotron community 15 years ago (Hignette *et al.*, 2001). Using a movable aperture at variable speeds, multiple iterations are needed to gradually approach a desired profile (Ziegler *et al.*, 2010; Peverini *et al.*, 2010). A precise mask may be more efficient than movable slits. IBF with masks has been reported previously (Gawlitza *et al.*, 2008). However, a method for precisely determining the ion beam distribution, the etching rate and the etching mask for suitable ion optics is lacking. In this short communication we remediate this gap and describe our method of preparing elliptical cylinder substrates for KB mirrors.

2. Methods

2.1. Experimental setup

A Kaufman KDC100 ion source was installed in a well of a large deposition system with linear transport as described previously (Liu *et al.*, 2003). The ion source was originally supplied with divergent dished optics, which was later reversed to a more suitable focused one. A mask support was built on top of the ion optics, with the sample moving over the mask opening (see Fig. 1).

2.2. Ion beam intensity distribution and mask aperture

A 127 mm-diameter Si wafer was painted with 13 parallel stripes, each ∼1 mm wide and spaced 7.5 mm apart, using colloidal graphite. The wafer was placed facing down on the mask holder with the stripes aligned perpendicular to the substrate moving direction. It was etched with an 800 V divergent beam for 10 min statically and cleaned in chemical solvents afterwards to remove the graphite. The un-etched stripe heights were measured every 5 mm along the central 100 mm region on every stripe using a stylus profiler. The measured step heights at the edges serve as calibration points to calculate the etching rates along the measured curve. The data were digitally processed to obtain the relative etch weighting on the mask. This process was repeated for the a 600 V focused beam.

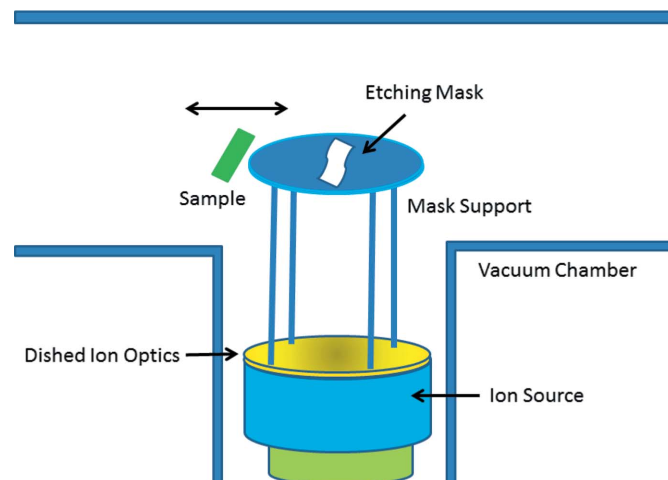

Figure 1
Schematic showing the basic setup of the profile-etching technique.

Parameters targeted for a nested KB pair are: a source-to-mirror distance of 5.7975 m, a mirror-to-focus distance of 0.2025 m and a mirror glancing angle of 3 mrad. An etching depth of 11 µm is needed for a 100 mm-long mirror. The etching depth is directly proportional to the length of the mask opening along the moving direction and the related etch weighting. By equating the summation of relative weighting to the required relative etching depth, the length of the opening can be determined relatively to a desired normalization length. This is the same methodology used in profile coating.

The ion intensity distribution and mask contour for both the divergent and focused ion beam are presented in Fig. 2. The divergent ion beam is broad and requires side shielding, while the focused beam passes mostly through the mask opening requiring no side shielding.

2.3. Etching procedures

It took many attempts to find the right procedure. Graphite masks and 1 mm-thick 100 mm × 12 mm Si stripes were used for test runs. For the divergent-beam test run, the surface profiles before and after etching were used to calculate the etching profile. This practice was challenging because the wafer would bend during etching. For the focused-beam test run, a graphite narrow stripe was painted along the wafer to use the step height as calibration to obtain the etching profile. The test results were scaled up to determine the total etching time for the final run, which was ~2 h for the 800 V divergent beam and ~1 h for the 600 V focused beam. The automated etching process, on flat Si substrates of 1 Å r.m.s. nominal roughness, involved multiple runs and 30 min breaks after each run. The gas pressure was 0.2 mTorr for the focused beam and 0.4 mTorr for the divergent beam. Metrology measurements were carried out using a micro-stitching interferometer (Assoufid *et al.*, 2007).

3. Results and discussions

Fig. 3 shows the measured profiles and the roughness data of divergent- and focused-beam-etched mirrors. The figure error and roughness r.m.s. values are 172 nm and 7.6 Å for the divergent beam and 48 nm and 1.5 Å for the focused beam, respectively. In Fig. 3(*a*) the spikes result from particulate contamination and the large figure error is caused by incorrect test runs. After a single profile etching using a focused beam a profile overlapping the ideal one was achieved, with a small figure error that can be corrected by profile coating. The results demonstrate the importance of correct calibration methods and optimized configurations to avoid side shielding. The surface roughness level of 1.5 Å r.m.s. could be further reduced by using other mask materials such as glass-like carbon that has less porosity compared with graphite.

The application of graphite stripes is critical for accurate ion figuring. This process solved the etching-induced bending problem as the step height is absolute and the measured etching profile is well defined with the bending curvature corrected. There are other methods to obtain the spatial profile of the ion beam, such as ion probes. These probes have to be calibrated at precise locations with bending problems considered.

The profile-etching technique is useful for correcting zonal figure errors where the etching depth along the sample is the same.

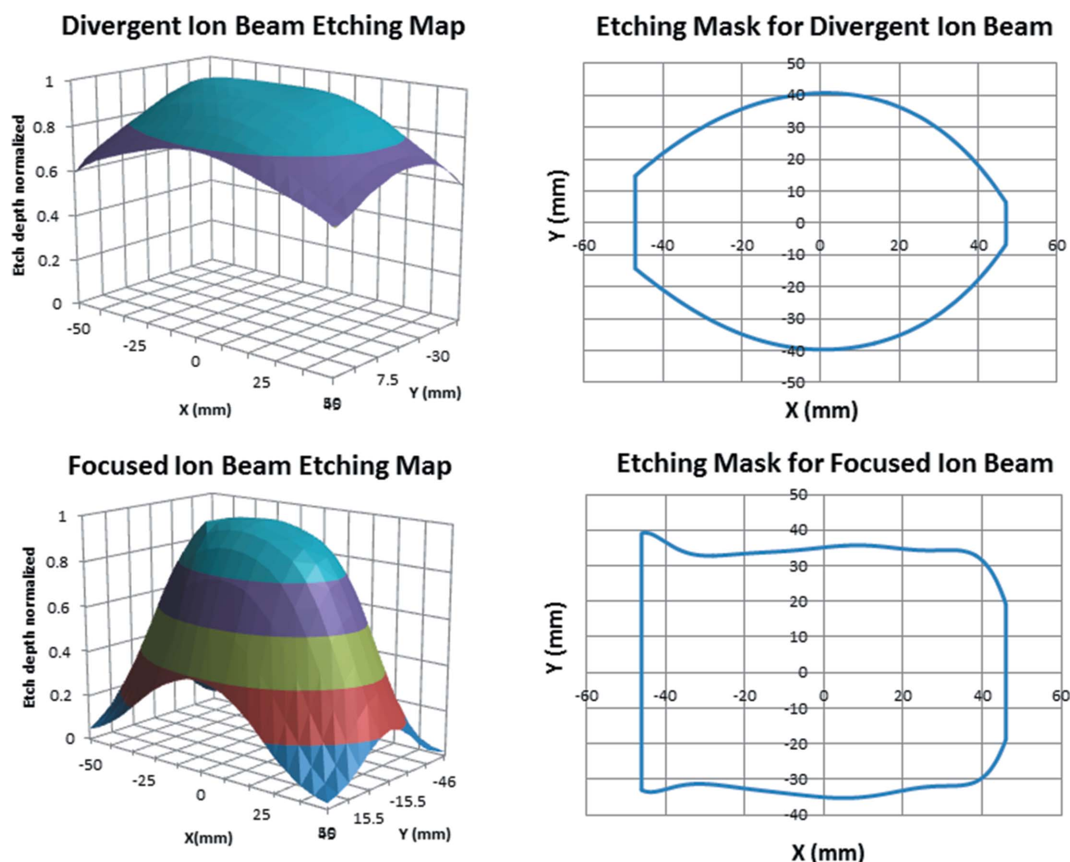

Figure 2
Ion beam intensity distribution maps and corresponding etching mask apertures for both divergent and focused ion optics as marked at the top of each figure. The sample moves along the Y axis with the etching profile along the X axis.

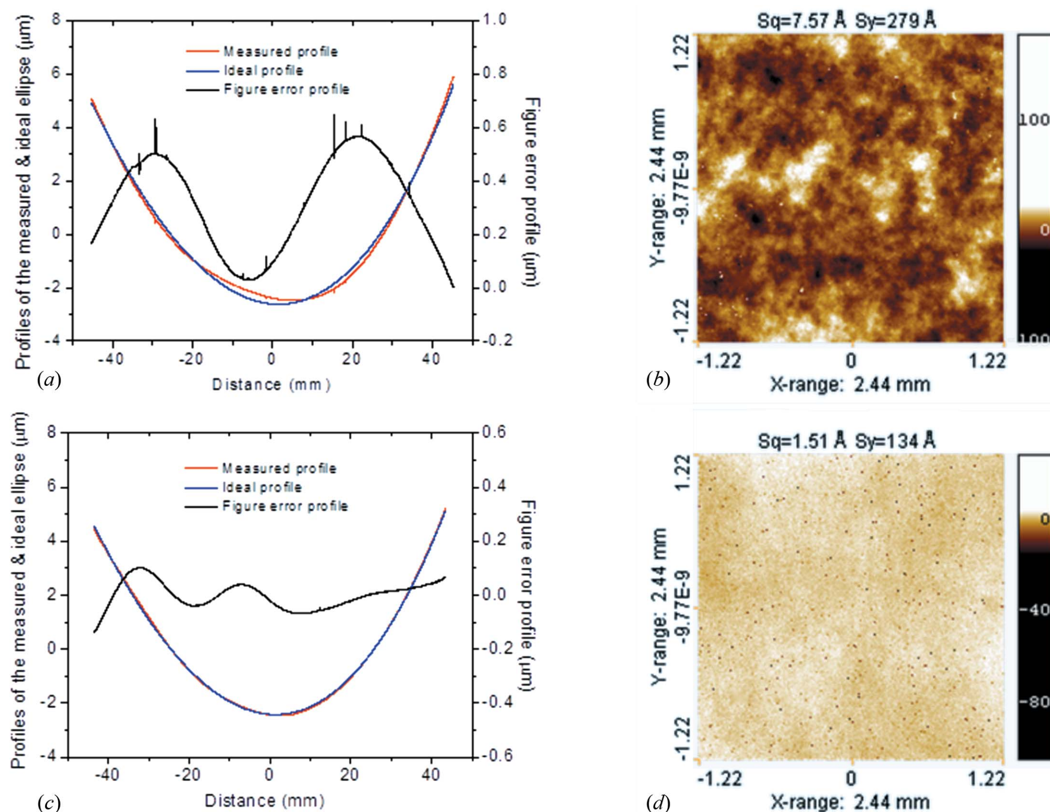

Figure 3
Measured elliptical profile (red) compared with the ideal (blue) for a profile-etched mirror using a divergent (*a*) and a focused (*c*) ion beam, and the corresponding roughness map for a divergent (*b*) and a focused (*d*) ion beam. S_q and S_y in (*b*) and (*d*) are r.m.s. and peak-to-valley roughness numbers, respectively, with bars on the right in units of Å.

Otherwise, a fine ion beam guided by in-place metrology feedback is needed.

A larger gap between the mask and the substrate is needed to avoid electrostatic pickup of debris in profile etching, which limits its ultimate accuracy. The figure error can be corrected by profile coating, however.

4. Conclusions

A technique for profile etching is presented in detail. A 100 mm-long elliptical KB mirror substrate with a 48 nm r.m.s. figure error and a 1.5 Å r.m.s. roughness was fabricated from a flat Si substrate using only one etching process at 600 V and 1 h total beam-on time. This technique combined with profile coating can be used to make precision KB mirrors with less coating and film stress. It can be used for single-layer and laterally graded multilayer nested KB mirrors, as well as other applications such as the figure correction of existing optics. Profile etching is relatively simple and fast, accurate and reliable, and can be applied without major investment in capital equipment.

We thank Elina Kasman, Michael Wieczorek and John Attig at Argonne National Laboratory for technical assistance. This work is supported by the US Department of Energy, Office of Science, Office of Basic Energy Sciences, under contract No. DE-AC02-06CH11357.

References

Assoufid, L., Qian, J., Kewish, C. M., Liu, C., Conley, R., Macrander, A. T., Lindley, D. & Saxer, C. (2007). *Proc. SPIE*, **6704**, 670406.

Gawlitza, P., Braun, S., Dietrich, G., Menzel, M., Schädlich, S. & Leson, A. (2008). *Proc. SPIE*, **7077**, 707703.

Hignette, O., Peffen, C., Alvaro, V., Chinchio, E. & Freund, A. A. (2001). *Proc. SPIE*, **4501**, 43–53.

Kang, H. C., Maser, J., Stephenson, G. B., Liu, C., Conley, R., Macrander, A. T. & Vogt, S. (2006). *Phys. Rev. Lett.* **96**, 127401.

Kewish, C. M., Guizar-Sicairos, M., Liu, C., Qian, J., Shi, B., Benson, C., Khounsary, A. M., Vila-Comamala, J., Bunk, O., Fienup, J. R., Macrander, A. T. & Assoufid, L. (2010). *Opt. Express*, **18**, 23420.

Liu, C., Assoufid, L., Conley, R., Macrander, A. T., Ice, G. E. & Tischler, J. Z. (2003). *Opt. Eng.* **42**, 3622.

Liu, C., Conley, R., Qian, J., Kewish, C. M., Liu, W., Assoufid, L., Macrander, A. T., Ice, G. E. & Tischler, J. Z. (2012*b*). *ISRN Opt.* **2012**, 151092.

Liu, C., Ice, G. E., Liu, W., Assoufid, L., Qian, J., Shi, B., Khachatryan, R., Wieczorek, M., Zschack, P. & Tischler, J. Z. (2012*a*). *Appl. Surf. Sci.* **258**, 2182–2186.

Liu, C., Macrander, A. T., Als-Nielsen, J. & Zhang, K. (2001). *J. Vac. Sci. Technol. A*, **19**, 1421.

Peverini, L., Kozhevnikov, I. V., Rommeveaux, A., Vaerenbergh, P. V., Claustre, L., Guillet, S., Massonnat, J.-Y., Ziegler, E. & Susini, J. (2010). *Nucl. Instrum. Methods Phys. Res. A*, **616**, 115–118.

Wen, H., Gomella, A. A., Patel, A., Lynch, S. K., Morgan, N. Y., Anderson, S. A., Bennett, E. E., Xiao, X., Liu, C. & Wolfe, D. E. (2013). *Nat. Commun.* **4**, 2659.

Ziegler, E., Peverini, L., Vaxelaire, N., Cordon-Rodriguez, A., Rommeveaux, A., Kozhevnikov, I. V. & Susini, J. (2010). *Nucl. Instrum. Methods Phys. Res. A*, **616**, 188–192.